J. Electroanal. Chem., 309 (1991) 273–292
Elsevier Sequoia S.A., Lausanne

Electrochemical charging of Pd rods

S. Szpak and C.J. Gabriel
Naval Ocean Systems Center, San Diego, CA 92152-5000 (USA)
J.J. Smith
Department of Energy, Washington, DC 20545 (USA)
R.J. Nowak
Office of Naval Research, Arlington, VA 22217-5000 (USA)

(Received 4 October 1990; in revised form 8 March 1991)

ABSTRACT

A model describing the electrochemical charging of Pd rods is presented. The essential feature of this model is the coupling of the interfacial processes with the transport of interstitials in the electrode interior. It is shown that boundary conditions arise from the solution of equations governing the elementary adsorption–desorption and adsorption–absorption steps and the symmetry of the electrode. Effects of the choice of rate constants of the elementary steps and the charging current on the surface coverage, the electrode potential and the time required to complete electrode charging are examined.

INTRODUCTION

In a recent effort [1] to account for the long charging time needed to initiate the effects reported by Fleischmann and Pons [2], in a Pd rod, certain assumptions concerning the concentration of deuterium at the electrode surface, the nature of the interaction between the diffusing deuterium and the Pd lattice and the homogeneity of the medium were made. The condition of zero flux at the center of Pd rod, used by Jorne [1], is evident; however, the condition of constant deuterium concentration at the electrode surface, although appropriate for charging from the gas phase, is open to question because, to be physically realistic, the boundary conditions must consider all processes that determine the concentration, or the flux, of the diffusing substance at the point where the influence of the interphase ceases. The nature of the interactions of diffusing hydrogen and, to a lesser degree deuterium, with the Pd lattice, has been examined in considerable detail [3–11]. To account for these interactions by a simple, first order irreversible chemical reaction may not be applicable. Moreover, a polycrystalline Pd rod can be treated as a homogeneous medium, but only under restrictive conditions.

The purpose of this work was to examine the problems associated with the charging of the palladium lattice. The charging of metals by hydrogen/ deuterium by itself is a technologically important issue aside from the interest generated by the recently described extraordinary behavior of deuterium charged Pd rods [2].

MODEL

Prior to developing the mathematics of the electrochemical charging of Pd rods, we review those aspects that tend to control the penetration of deuterium. In particular, we examine the structure of the

electrolyte/electrode interphase, the deuterium evolution reaction, interactions between the interstitials and the host lattice, and the effect of grain boundaries in the polycrystalline material. This qualitative discussion provides the basis for the formulation of simplified governing equations in which we ignore the distinction between α/β phases and employ a simple diffusion coefficient for the purpose of modeling the coupling between surface and transport (bulk) processes.

Concept of an Interphase/Charging Fluxes

Two homogeneous phases that are in contact with each other are separated by an interphase region. This region may be viewed as made up of several laminae each of which is treated as a very thin homogeneous phase [12]. Often, to simplify the treatment, an appropriately defined single homogeneous phase may be substituted [13]. The structure of the electrolyte portion of the interphase was treated by van Rysselberghe [14]; here, the structure on the metal side, with respect to transport, will be identified and examined.

Four fluxes are involved in charging the Pd metal from the gas phase. They are the adsorption and desorption fluxes, j_2 and j_{-2}, and the absorption–desorption fluxes consisting of the exchange between the species present in the metal interior and the surface, j_3 and j_{-3}, respectively. In reality, the dynamics of the surface processes are more complex [15,16]. In the case of electrochemical charging, Fig. 1, the structure is complicated further because the applied overpotential and charge transfer result in two additional fluxes, j_1 and J_{-1}. The effect of the applied potential on the transport of interstitials becomes negligible at a point close to the metal surface where diffusion is initiated.

Deuterium Evolution Reaction

The reaction path for the deuterium evolution is essentially the same as that for hydrogen [2,17], eqns. (I) to (III)

$$D_2O + e^- \rightarrow D(a) + OD^- \qquad k_1, k_{-1}, \eta \tag{I}$$

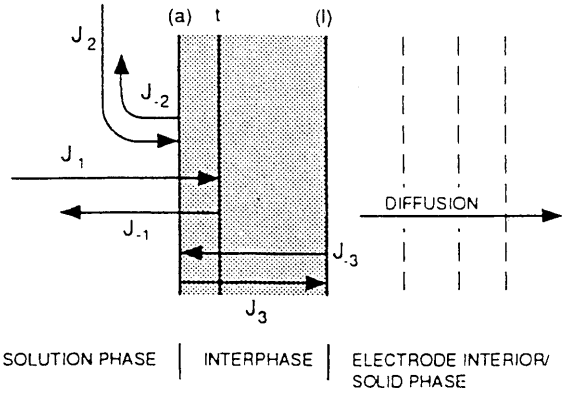

Figure A-1. Schematic representation of an interphase (fluxes included). (a) Adsorption plane; (t) charge transfer plane; (l) lattice.

followed by either

$$D_2O + D(a) + e^- \rightarrow D_2(s) + OD^- \qquad k_2, k_{-2}, \eta \tag{II}$$

or

$$D(a) + D(a) \rightarrow D_2(s) \qquad k_3, k_{-3} \tag{III}$$

where (a) and (s) denote species present in an adsorbed state and in solution, respectively. Potential dependent surface coverage for special cases, e.g., the steady state condition with an a priori specified rate determining step (rds), in the absence of absorption, was examined by Gileadi and Conway [18]. They found that highest surface coverages are obtained when eqn. (III) is the rds, i.e., is proceeding more rapidly than eqn. (II), but more slowly than eqn. (I). Furthermore, if eqn. (II) is the rds, i.e., is proceeding more rapidly than eqn. (III), but more slowly than eqn. (I), the surface coverage exhibits a limiting value, determined by the ratio k_2/k_1; the smaller this ratio, the higher the surface coverage.

The absorption into the lattice of electrochemically generated deuterium is given by eqn. (IV)

$$D(a) \rightarrow D(1) \qquad k_4, k_{-4} \tag{IV}$$

where (l) denotes species in the lattice. The hydrogen analog of eqn. (IV) was investigated to a limited extent by Iyer et al. [19]. The inclusion of diffusional transport necessitates the separation of the interphase region from the diffusion space. The characteristic feature of the Iyer et al. model is the interdependence of the diffusion flux and the interphase reactions.

Molecular Interactions Related to Transport

There is ample experimental evidence of interactions between the interstitials and the host Pd lattice. During the transport of hydrogen as well as deuterium, a change from the α phase to the β phase occurs. This change manifests itself by the lattice expansion which is larger in the α phase than in the β phase [6]. The expansion of the Pd lattice creates localized highly stressed conditions that affect the diffusional transport [10]. This deviation from ideality occurs even at very low hydrogen concentration with the process becoming more exothermic as the concentration of H(l) increases. However, once the β phase has formed, the process becomes less exothermic. The rate of absorption increases exponentially with the increase in H(l) concentration and is attributed to an expansion of the lattice.

Quantum mechanical treatment requires that the motion of interstitials occurs by a hopping mechanism [9]. The energies of activation for the H/D species are of an order of magnitude less than for other interstitials, while the values of their diffusion coefficients are many orders of magnitude higher indicating the importance of the pre–exponential factor. The jump frequencies for H interstitials are comparable to the highest frequency of the host lattice. Of interest is the fact that the isotope effect enters through the exponential factor, i.e., contrary to the prediction based on the classical absolute rate theory [15].

Forms of Diffusion Coefficient

Here, we review the various interpretations of the diffusion coefficient to underscore the importance of interactions between the interstitials and the host lattice on their transport. Starting with the Fick's first law, eqn. (1)

$$j = -\boldsymbol{D}\frac{\partial c}{\partial x} \tag{1}$$

we note that in this formulation, **D** is a proportionality constant relating the flux, j, to the driving force, $\partial c/\partial x$. However, as written, eqn. (1) is valid only for non–interacting solute/ solvent systems. Substituting the activity for concentration, $a = c\phi$, we transform eqn. (1) into an equivalent form

$$j = \frac{c\boldsymbol{D}}{RT}\frac{\partial \mu}{\partial x} \quad \mu - \mu^0 + RT \ln a \tag{2}$$

Defining $\upsilon = j/c$ as the average linear velocity of the diffusing particles, we have for the Nernst–Einstein formulation

$$f(x)dx = B^{-1}\upsilon dx \quad B = \boldsymbol{D}/RT \tag{3}$$

i.e., the diffusing particles behave as if they were acted upon with the force *f(x)* against the viscous resistance. If additional forces are affecting diffusional transport, e.g., lattice expansion, it is necessary to add the appropriate terms to the balance eqation, eqn. (3), e.g., eqn. (4)

$$f(x)dx = B^{-1}\upsilon dx + \sum_i d\omega_i \tag{4}$$

Comparing eqns. (3)/(4) and (2) we note that f(*x)* = —$\partial\mu/\partial x$ while the comparison of eqns. (1) and (2) yields the diffusion coefficient of the form

$$\boldsymbol{D} = \boldsymbol{D}_0 \exp\left[-\frac{1}{RT}\int\left[f(x) - \sum_i d\omega_i/dx\right]dx\right] \tag{5}$$

Equation (5) implies that the diffusion coefficient reflects specific features associated with the transport. For example, Barrer and Jost [20] found that the transport of H(l) in the Pd lattice belongs to the "zeolitic diffusion", where the probability of migration is proportional to the probability of finding an unoccupied site. The diffusion coefficient involving the possibility of jumps of length λ over several sites has the form

$$\boldsymbol{D}_n = (n\lambda)^2(1-\zeta)^n\nu \exp(-E_n/RT) \tag{6}$$

where ν is the oscillation frequency, $(1-\zeta)^n$ is the probability of finding a vacant neighboring site *n* times in succession and E_n is the energy of activation, most likely a slowly varying function of *n*. The "effective" diffusion coefficient D_{eff} is the normalized sum of individual coefficients. Evidently, for small ζ, the *n*–fold jumps contribute substantially while for large ζ only the first term is significant.

Kuballa and Baranowski [21], examining the transport properties at high con– centration of hydrogen through the β – Pd lattice, employed the diffusion coefficient formulated on the basis of absolute rate theory, eqn. (7)

$$\boldsymbol{D} = \kappa f\frac{\lambda^2}{6}z\nu \exp\left(\frac{S_m + S_f}{k}\right)\exp\left(-\frac{E_m + E_f}{kT}\right) \tag{7}$$

where ϰ is the transmission coefficient, *f* is the correlation factor, λ is the jump distance in the lattice, *z* the coordination number, ν the vibration frequency in the potential well, *S* the entropy and *E* the energy. The subscripts f and m, respectively, identify the formation of a neighboring vacancy and the motion from one site to another. They concluded that within the phase, the diffusion coefficient is independent of concentration. However, at higher concentrations, many neighboring sites are occupied and both the entropy and the energy of vacancy formation must be included. The formation of new sites is associated with the mechanical distortion of the lattice, thus sharply increasing the vibrational frequency of the diffusion particle. As the concentration of hydrogen increases there is continuous change in the mechanism of transport, most likely involving the tetrahedral sites.

In yet another example, the effect of mechanical distortion on transport was examined by Voelkl [10]. Results were expressed in terms of changes of the electrochemical potential, i.e. a factor appearing in the exponent of the diffusion coefficient.

Effect of gra in boundaries

Grain boundaries represent the locations of a high density of lattice imperfections. In effect, they may be viewed as internal surfaces where an exchange process,

similar to adsorption–desorption, can occur. The interaction of an interstitial with a lattice defect is energetically quite different from its interaction with the undisturbed lattice. Consequently, by eqn. (5), transport properties should differ in polycrystalline material as compared with those in a single crystal. Yet, measurements of the steady state permeation of hydrogen indicate no influence of grain boundaries. This apparent discrepancy is attributed to the absence of trap–to–trap hopping of interstitials and the filling of all traps during steady state transport [22]. By creating sinks, the tendency of interstitials to accumulate in the lattice defects modifies their transport before the steady state is realized.

H(a) / H(l)–Pd Vs. D(a) / D(l)–Pd Interphase Behavior

Common reaction paths for the hydrogen evolution reaction and deuterium evolution reaction, reported by Schuldiner and Hoare [17], do not assure identical rates of the elementary process comprising the charging of palladium rods. Qualitative observations show considerable difference in the behavior of the interfacial region between hydrogen and deuterium, notably in the rate of absorption–desorption. Rolison and Trzaskoma [23] reported a significant difference in the rate of escape of absorbed hydrogen and deuterium upon termination of the charging current. Szpak et al. [24] found similar behavior by an in situ examination of the penetration of deuterium and hydrogen by a single grain in a specially designed cell using Nomarski optics.

FORMULATION OF CHARGING EQUATIONS

Davenport et al. [25] considered absorption from the gas phase into a thin metallic film. We extend their treatment to consider a much larger solid body immersed in an electrolyte. This body is taken to consists of N layers; the i th layer having a volume V_i and the area of the dividing surface between it and the $(i + 1)$th layer is $S_{i,i+1}$. In general: $V_i \neq V_{i+1}$ and $S_{i-1,i} \neq S_{i,i+1}$. The diffusion of deuterium in the bulk of the solid body is then considered as a process of jumping from one layer to an adjacent layer with a rate that is proportional to the interfacial area between the layers, as well as to the number of occupied sites in the initial layer and the number of vacant sites in the final layer. Consequently, we write for the time rate of change in the fractional number per unit volume of occupied sites, ς_i in the *i*th layer within the bulk

$$\frac{d\zeta_i}{dt} = \frac{\kappa_d Z_m}{V_i}\Big\{ S_{i\text{-}1,i}\big[\zeta_{i\text{-}1}(1-\zeta_i) - \zeta_i(1-\zeta_{i\text{-}1})\big] - S_{i,i+1}\big[\zeta_i(1-\zeta_{i+1}) - \zeta_{i+1}(1-\zeta_i)\big]\Big\} \quad i = 1, 2, 3, ..., N \tag{8}$$

where k_d is the jump rate constant and Z_m is the maximum number of available sites per unit volume.

The boundary conditions for this set of equations are determined by the physical considerations of events occurring at the first and Nth layers. The reactions (I) through (IV) set the boundary conditions at the first layer in terms of corresponding fluxes. Defining the anodic current as the positive current (i.e., the flow of electrons from the working electrode to the power supply), we obtain for the charge transfer reaction, eqn. (I)

$$\frac{i_1}{T_m F} = k_{-1} OD^-]\theta \exp\left(\frac{\alpha F\eta}{RT}\right) - k_1[D_2O](1-\theta)\exp\left[\frac{-(1-\alpha)F\eta}{RT}\right] \tag{9}$$

where Γ_m, is the maximum number of sites per unit area and θ is the fractional surface coverage. Analogously, for the charge transfer reaction eqn. (II)

$$\frac{i_2}{T_m F} = k_{-2}[D_2(s)][OD^-](1-\theta)\exp\left(\frac{\beta F\eta}{RT}\right) - k_2[D_2O]\theta\exp\left[\frac{-(1-\beta)F\eta}{RT}\right] \tag{10}$$

While reactions (III) and (IV) do not directly pass electrons through the interface, it is convenient to define equivalent charge transfer currents, eqns. (11) and (12), respectively

$$\frac{i_3}{T_m^2 F} = 2k_{-3}[D_2(s)](1-\theta)^2 - 2k_3\theta^2 \tag{11}$$

$$\frac{i_4}{T_m Z_m F} = k_{-4}\zeta_1(1-\theta) - k_4\theta(1-\zeta_1) \tag{12}$$

In terms of these currents, the time rate of change of adsorbed deuterium is given by eqn.(13)

$$T_m F\frac{d\theta}{dt} = -i_1 + i_2 + i_3 + i_4 \tag{13}$$

and the applied current, *i*, is given by eqn. (14)

$$i = i_1 + i_2 + C\frac{d\eta}{dt} \tag{14}$$

where the last term in eqn. (14) gives the charging current for the interfacial layer in terms of its effective capacitance *C* and the time rate of change of the overpotential. The time rate of change of the absorbed deuterium in the interfacial layer between the bulk Pd and the electrolyte is governed by both the flux through the surface given in terms of the equivalent current i_4 and diffusion into the bulk, which generates the flux: $k_d Z_m^2 S_{1,2}[\zeta_1(1-\zeta_2) - \zeta_2(1-\zeta_1)]$, so that the time rate of change of the fractional occupation of sites in the interfacial layer is given by eqn. (15)

$$V_1 Z_m\frac{d\zeta_1}{dt} = -S_{0,1}\frac{i_4}{F} - d_d Z_m^2 S_{1,2}(\zeta_1 - \zeta_2) \tag{15}$$

Equations (13), (14) and (15) specify, in effect, the boundary conditions for eqn. (8) at the interfacial layer. The boundary condition at the Nth layer depends on the physical arrangement; e.g., with reflection symmetry at that location, the flux passing beyond the Nth layer would be zero.

The jump rate constant k_d introduced in eqn. (8) can be related to the diffusion constant by observing that, if the number of layers is large and each layer is thin, then eqn. (8), which in cartesian coordinates becomes

$$\frac{d\zeta_1}{dt} = \frac{k_d Z_m}{\delta}(\zeta_{i-1} - 2\zeta_i + \zeta_{i+1} \tag{16}$$

where δ is the thickness of the layers, can be compared with the finite difference approximation to the diffusion equation indicating that the diffusion constant $\mathbf{D} = k_d Z_m \delta$.

Charging of Pd Rods; Numerical Solutions

For a rod (cylindrical symmetry) divided into annular layers of thickness Δr numbered from surface to center (1 to N), eqn. (8) becomes eqn. (17) (see Appendix)

$$\frac{d\zeta_i}{dt} = \frac{k_d Z_m}{\Delta r}\left(\frac{2r_i}{r_i + r_{i+1}}\right)\left[\zeta_{i-1} - \left(2 - \frac{\Delta r}{r_i}\right)\zeta_i + \left(1 - \frac{\Delta r}{r_i}\right)\zeta_{i+1}\right] \quad i = 2,3,4,\ldots,N \tag{17}$$

where $r_i = (N - i + 1)\Delta r$ and $\zeta_{N+1} = \zeta_N$ in order to insure the condition of zero flux at the center of the rod as required by symmetry considerations. Similarly, for the interfacial layer between the electrolyte and the bulk, eqn. (15) becomes eqn. (18)

$$= -\left(\frac{2r_0}{2r_0 - \Delta r}\right)\left\{\frac{T_m}{\Delta r}\left[k_{-4}\zeta_1(1-\theta) - k_4\theta(1-\zeta_1)\right] + \frac{k_d Z_m}{\Delta r}\left(\frac{r_0 - \Delta r}{r_0}\right)(\zeta_1 - \zeta_2)\right\} \tag{18}$$

where $r_0 = N\Delta r$ is the radius of the rod.

Equations (13), (14), (17) and (18) form a set of stiff ordinary differential equations that can be solved using e.g. the method of Kaps–Rentrop described by Press and Teukolsky [26] with suitable modifications to take advantage of the tridiagonal nature of the Jacobi matrix.

RESULTS AND DISCUSSION

A proposed requirement for the initiation of the effect reported by Fleischmann and Pons is that a set of conditions must be met to “switch–on” the Pd electrode. Due to a large number of these conditions it is difficult, if not impossible at the present time, to identify a dominant factor although a high degree of loading has

been assumed to be one of the necessary conditions. High overpotentials and/or charging currents have also been proposed. In the context of the present discussion, we accept the correctness of the reaction path, eqns. (I)—(IV). However, because of the lack of the rate constant data for the deuterium evolution reaction, the discussion is essentially reduced to the examination of the behavior of the set of coupled equations describing the charging process.

Construction of Solution; Input Data

The numerical solution of eqns. (13), (14), (17) and (18) requires three types of input parameters. The first is associated with the electrode/electrolyte system, the second characterizes the initial conditions, and the third comprises the rate con– stants whose effect on charging process is examined. The electrode/electrolyte system consists of two regions: (i) the bulk material characterized with regard to transport by the density of available bulk sites, Z_m, and the diffusion coefficient **D**; (ii) the electrode/electrolyte interface described by the density of available surface sites, Γ_m, and the rate constants for all processes including the exchange reaction, eqn. (IV). The assumption employed here of concentration independent parameters represents a first approximation only, but can be easily extended to incorporate concentration dependences, if they are known.

To initiate calculations, we assume that, prior to the application of a charging current, equilibrium has been reached so that the time rate of change of η, θ, and ζ_i = 1,2, 3... , N will be zero; in addition, we require that the time rate of change of the evolution of $D_2(s)$ also be zero. The latter requirement imposes the condition that $i_2 + i_3 = 0$. Consequently, the equilibrium condition becomes $i_j = 0$; j = 1,2,3,4. Equilibrium is characterized by the values of the three variables: η, θ, and $\zeta = \zeta_i$; i = 1,2, 3,... N and determined by four equations. It follows, therefore, that an equilibrium condition may not exist for arbitrarily chosen sets of rate constants for the four reactions, eqns. (I)—(IV). For this reason, it is convenient to choose equilibrium values for θ and ζ with $\eta = 0$, viz., $\theta = \theta_0$, $\zeta = \zeta_0$ and use these values to provide the following relationships among the rate constants, eqns. (19)—(22)

$$k_{-1}[OD^-]\theta_0 = k_1[D_2O](1 - \theta_0) \tag{19}$$

$$k_{-2}[D_s(s)][OD^{-1}](1 - \theta_0) = k_2[D_2O]\theta_0 \tag{20}$$

$$k_{-3}D_2(s)](1-\theta_0)^2 = k_3\theta_0^2 \tag{21}$$

$$k_{-4}\zeta_0(1-\theta_0) = k_4(1-\zeta_0)\theta_0 \tag{22}$$

Table 1 lists the values of the parameters used in the computations described here unless noted otherwise.

Table A-1. Input data.

Parameter	value
$[D_2O]$	5.5×10^{-2} mol/cm^3
$[OD^-]$	1.0×10^{-4} mol/cm^3
$[D_2(s)]$	8.3×10^{-7} mol/cm^3
θ_0	1.0×10^{-1}
ζ_0	1.0×10^{-1}
α	5.0×10^{-1}
β	3.0×10^{-1}
Z_m	1.0×10^{-1} mol/cm^3
Γ_m	1.0×10^{-13} mol/cm^2
radius, r_0	5.0×10^{-3} cm
capacitance, C	4.0×10^{-3} F/cm^2
diff. coeff., D	1.0×10^{-5} cm^2/s
Number of layers, N [a]	10

[a] Calculations for $N > 10$ (e.g. $N = 40$) yielded substantially the same results.

Electrode Charging

To relate the charging process to observable quantities and to evaluate the driving force, we calculated the surface coverage, the electrode overpotential and the amount of absorbed material. In particular, the surface coverage was selected because the operating driving force for the charging process is the chemical potential difference between the relevant species in an adsorbed state and those residing in the lattice. For the charging process to occur we require that the inequality, eqn. (23)

$$\mu(a,t) - \mu(l,t) > 0 \tag{23}$$

be fulfilled at all times. But, since $\mu(a, t) = f_1(\theta)$ and $\mu(l, t) = f2(\zeta)$, it follows that the charging process may be conveniently examined in terms of the surface coverage which is determined by the participating processes responding to the applied charging current. The amount of material incorporated into the electrode interior and its distribution was calculated to determine whether or not a threshold value for loading has been reached and to provide information on the efficiency of the charging process.

An example of an electrode charging is shown in Fig. 2 where two time intervals are delineated. The first is of a short duration, e.g., less than 0.1 s, during which the processes within the interphase dominate. This period terminates when these processes become stationary, i.e. as $\theta(t) \rightarrow \theta_{lim}$ and $\eta(t) \rightarrow \eta_{lim}$. The second time interval, of a considerable length, is that during which actual charging of the electrode interior occurs, i.e., the fraction of available sites occupied $Q(t) \rightarrow Q_{lim}$.

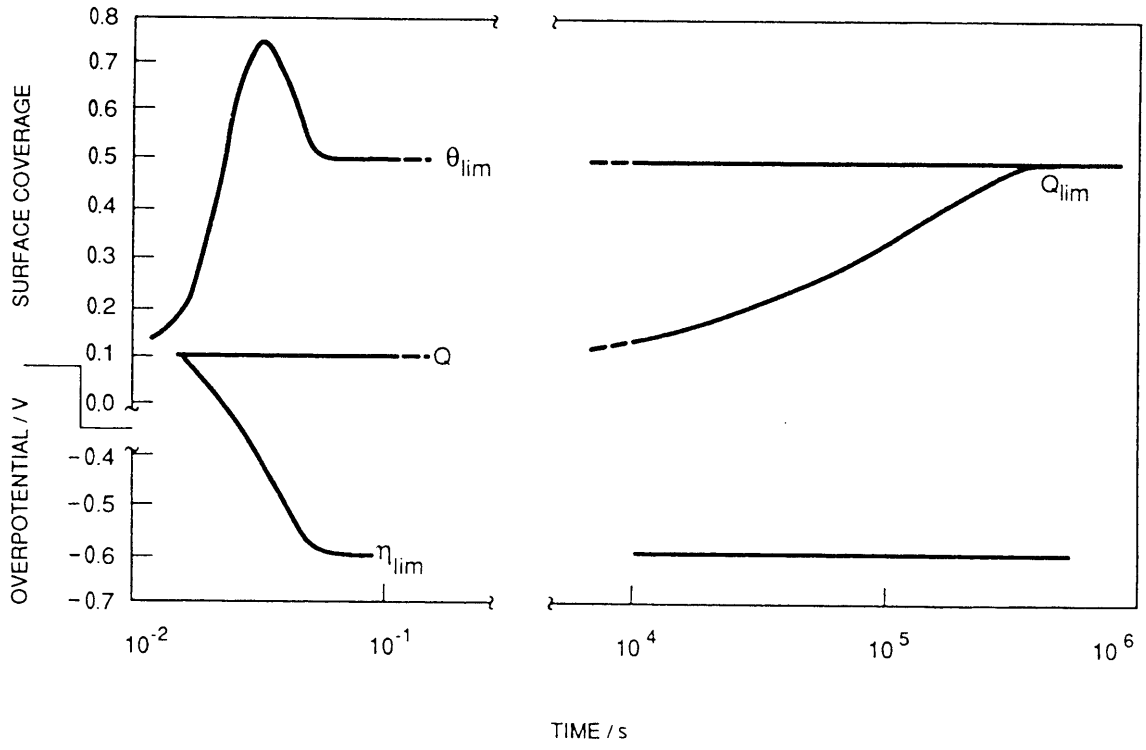

Figure A-2. Evolution of surface coverage, overpotential and concentration of interstitial in the course of electrode charging.

Electrode Initial Response to Current Flow

The assumed model, Fig. 3, provides for position dependent elementary processes, i.e., it suggests the separation of processes occurring within. the interphase from those within the electrode interior. It follows that the electrode charging and the effect of rate constants can be examined within well defined time intervals, as illustrated in Fig. 2, of which the first time interval consists of three distinct time periods: the first, $0 < t < \tau_1$, represents the charging of the double layer; the second, $\tau_1 < t < \tau_2$, covers the period needed for the attainment of a quasi–stationary state; and the third $t > \tau_2$ is the time during which the electrode begins to accept interstitials, Fig. 3. For different choices of rate constants, the regions may be less distinct and the time dependence of the surface coverage and overpotential can have somewhat different forms. The amount of the interstitial material absorbed during the attainment of the quasi–steady state of surface coverage is insignificant under all conditions examined (e.g., on the order of 0.0001% above the assumed equilibrium value).

As expected, an elementary process that controls the overall reaction also controls the time dependence of both the surface coverage and overpotential. In particular, Fig. 4 illustrates the effect of an emerging rds. Here, the pairs of curves, respectively, a—a′, b—b′, etc. are the $\theta(t)$ and $\eta(t)$ that represent changes in the surface coverage and overpotential with the changing ratios of k_2/k_1 and k_3/k_1. Clearly, as these ratios are decreased, the quasi–steady state surface coverage, θ_{lim}, increases due to enhanced adsorption and reaches a limiting value of one. Further decrease in this ratio, after $\theta_{\text{lim}} = 1.0$, causes the knee of the $\theta(t)$ curve to move to earlier times, cf. curves c and d. It is noted that within the time period examined, the amount of absorption is insignificant; consequently, as expected, an agreement with the earlier work of Gileadi and Conway [18] is evident.

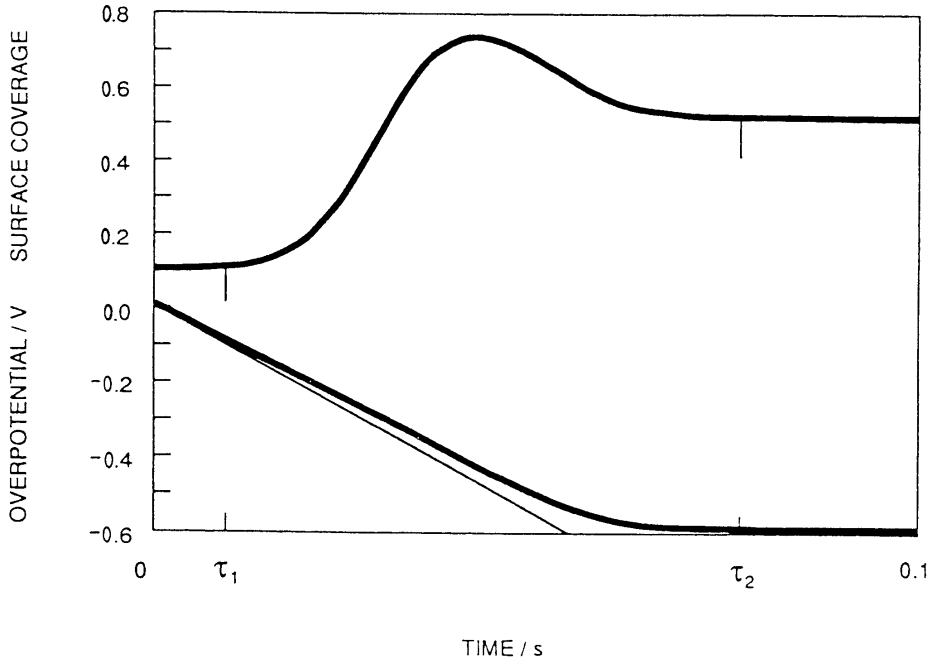

Figure A-3. Surface coverage and overpotential as a function of time. Initial period: charging of the double layer, $0 < t < \tau_i$; unsteady state, $\tau_1 < t < \tau_2$; quasi-steady state, $t > \tau_2$. Charging current: -40×10^{-3} A/cm^3; rate constants: $k_1 = 10^3$ cm^3/mol s; $k_2 = 10$ cm^3/mol s; $k_3 = 10^3$ cm^2/mol s; $k_4 = 2.0 \times 10^5$ cm^3/mol s.

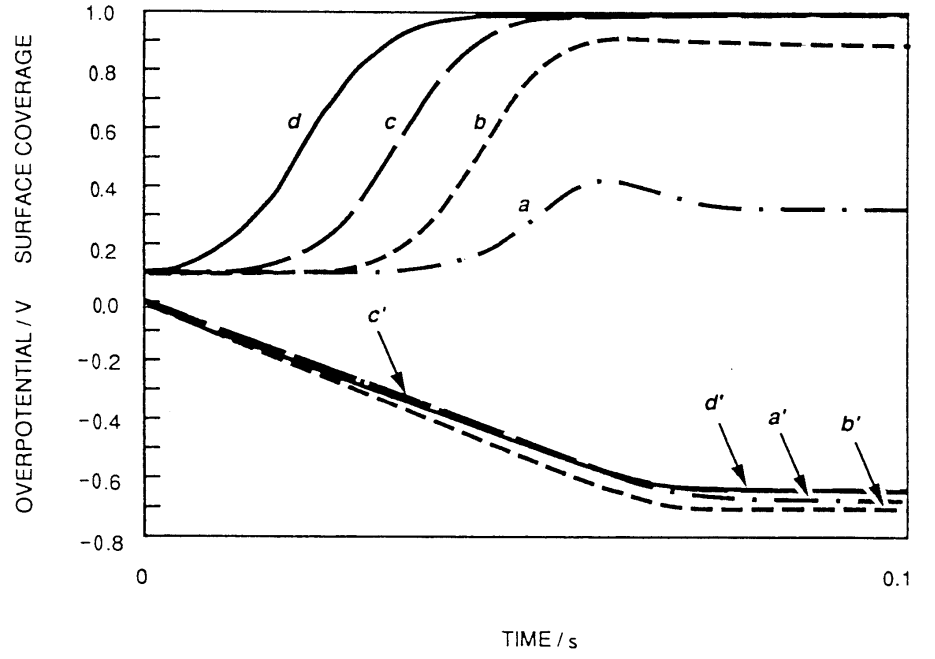

Figure A-4. Surface coverage and overpotential as a function of time. Effect of an emerging rds. Charging current: -40×10^{-3} A/cm^2; rate constants: $k_2 = 1.0$ cm^3/mol s, $k_3 = 0.1$ cm^2/mol s, $k_4 = 3 \times 106$ cm^3/mol s; $k_1 = 10^2$, 10^3, 10^4, 10^5 cm^3/mol s for curves a, b, c, and d, respectively.

A somewhat different behavior is seen as the rds is changed from the recombination reaction, Fig. 5 curve a, to electrodesorption, Fig. 5 curve b. The effect, which is minimal in the $\theta(t)$ curve, is associated with a more negative overpotential, decreased by ca. 200 mV and a longer time required to attain the quasi–steady state. This is likely connected with the fact that the recombination reaction does not involve charge transfer.

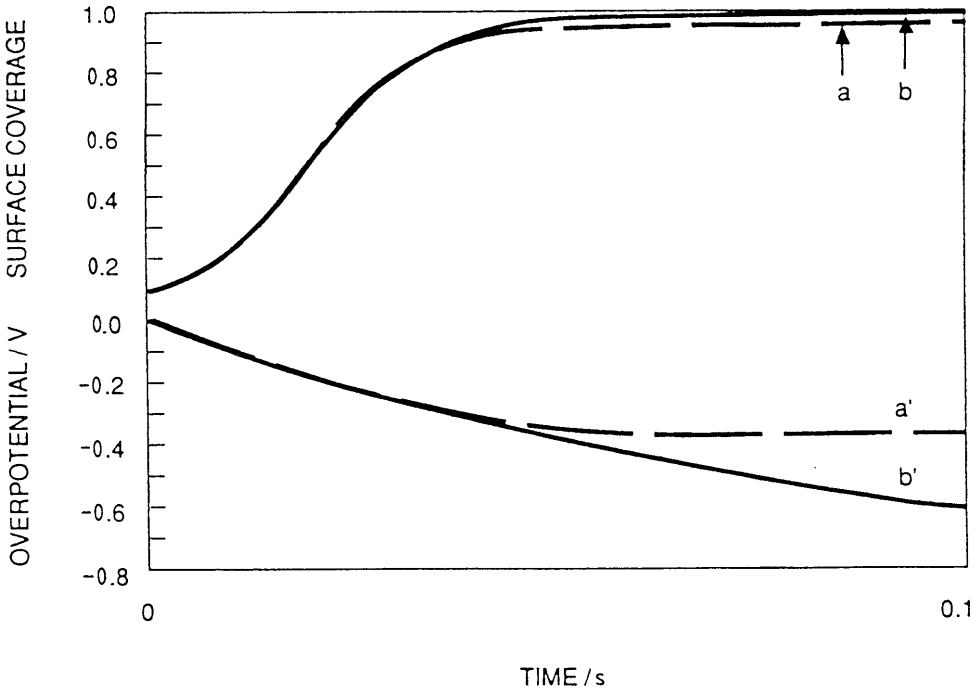

Figure A-5. Surface coverage and overpotential as a function of time. Effect of changing the rds. Charging current: -40×10^{-3} A/cm^2; $\theta_0 = 0.1$; $\zeta_0 = 0.08$. Rate constants: $k_1 = 10^6$ cm^3/mol s, $k_4 = 2.0 \times 10^7$ cm^3/mol s. (a) $k_2 = 1.0$ cm^3/mol s, $k_3 = 10^3$ cm^2/mol s (b) $k_2 = 10^3$ cm^3/mol s, $k_3 = 1.0$ cm^2/mol s.

Intuitively, the present model ascribes a dominant role to the rate of absorption, viz., the higher the rate, the faster the charging of the electrode. However, due to coupling between the surface processes, no such clear conclusion should be drawn unless the interphase (j_3, j_{-3}) controls the overall event. In general, an increase in the rate of absorption shifts the attainment of the quasi–steady state to somewhat longer times, as illustrated in Fig. 6. Also, the lower the rate of absorption, the greater the tendency to develop a maximum in the $\theta(t)$ curve, Fig. 6, curve a.

The coupling effect of the interphase processes on the surface coverage and overpotential as a function of charging current, suggested by eqns. (13) and (14), is illustrated in Figs. 7–9. Here, three cases are illustrated, viz., with the electrodesorption reaction as the rds, θ_{lim} increases with an increase in the charging current, Fig. 7; with a less clearly defined rds, θ_{lim} first increases, goes through a maximum and then decreases, Fig. 8; and with recombination/adsorption as a rather weak rds, θ_{lim} always decreases with an increase in the charging current, Fig. 9.

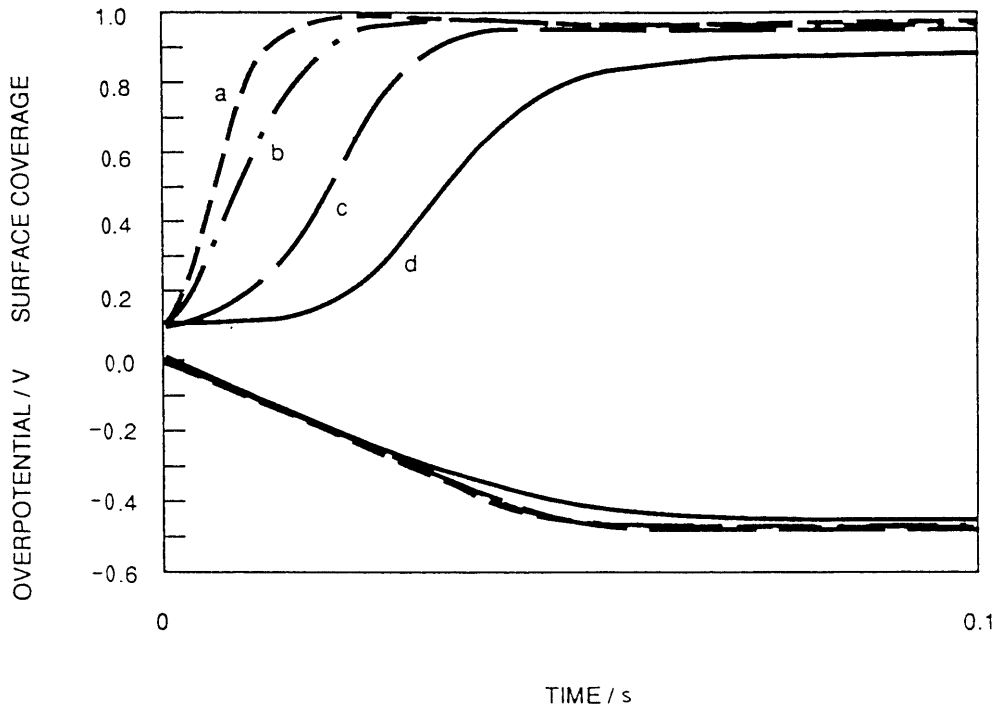

Figure A-6. Surface coverage and overpotential as a function of time. Effect of adsorption-absorption exchange rate. Charging current: -40×10^{-3} A/cm^2. Rate constants: $k_1 = 10^5$ cm^3/mol s, $k_2 = 100$ cm^3/mol s. k_3 = (a) 3.0×10^4, (b) 3.0×10^5, (c) 3.0×10^6, (d) 3.0×10^7 cm^3/mol s.

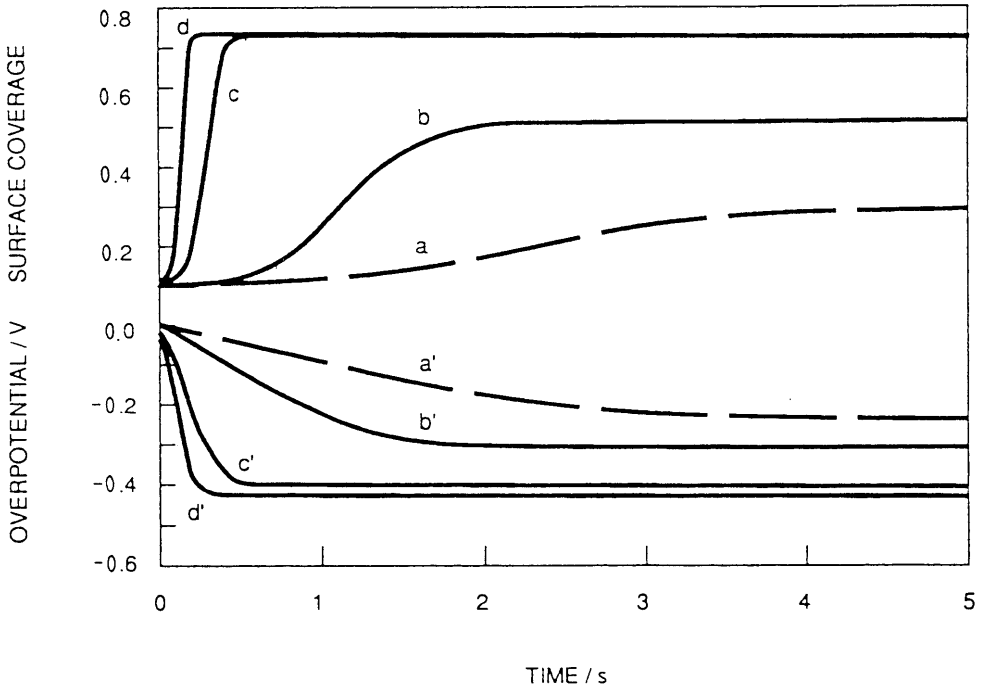

Figure A-7. Surface coverage and overpotential as a function of time. Effect of charging current. Rate constants: $k_1 = 105$ cm^3/mol s, $k_2 = 10^3$ cm^3/mol s. $k_3 = 1.0$ cm^2/mol s, $k_4 = 2.0 \times 10^7$ cm^2/mol s. Charging current: (a) -4.0×10^{-3}, (b) -10.0×10^{-3} cm^3/mol s, -40.0×10^{-3}, (d) -80×10^{-3} A/cm^2.

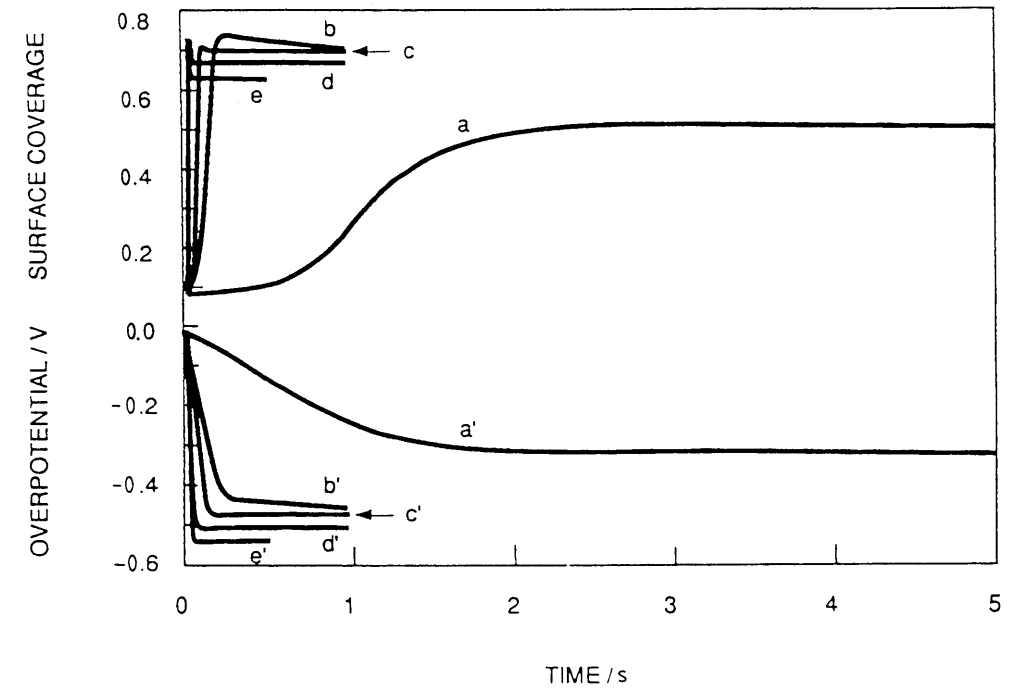

Figure A-8. Surface coverage and overpotential as a function of time: Effect of charging current. Rate constants: as in Fig 6. except for k_3 = 10.0 cm^2/mol s. Charging current: (a) –10.0 × 10^{-3}, (b) –40.0 × 10^{-3}, (c) –80.0 × 10^{-3}, (d) –160.0 × 10^{-3}, (e) –800.0 × 10^{-3} A/cm^2.

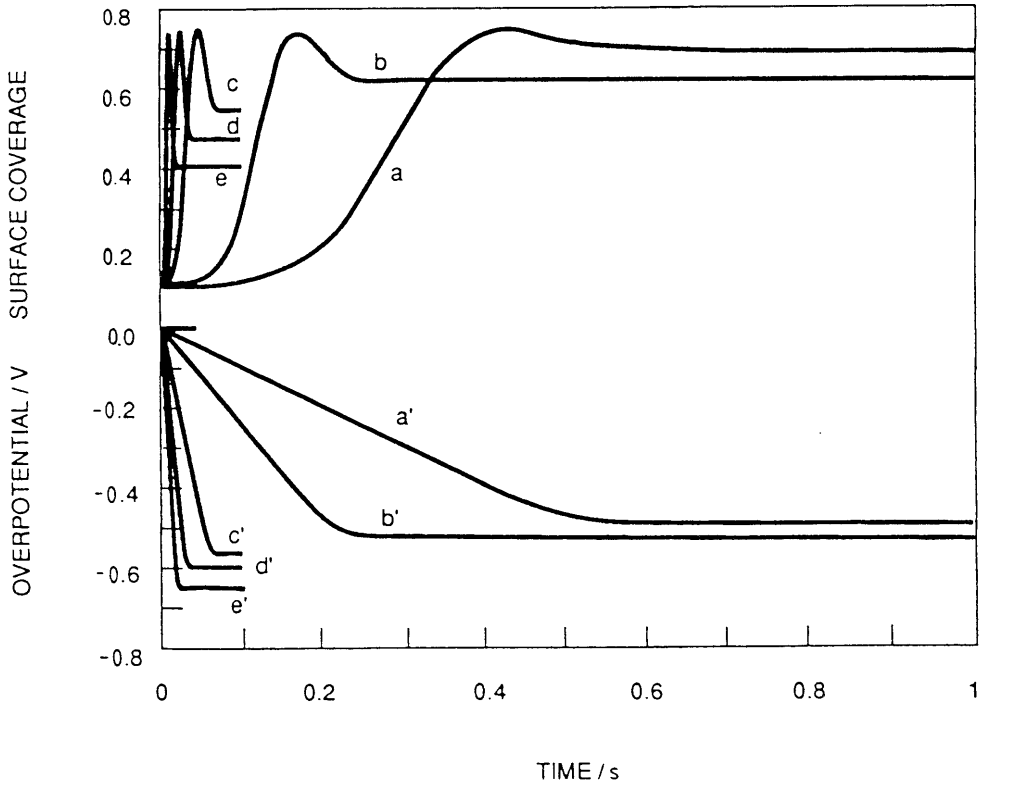

Figure A-9. Surface coverage and overpotential as a function of time: Effect of charging current. Rate constants: k_1 = 1000 cm^3/mol s, k_2 = 10 cm^3/mol s, k_3 = 1000 cm^2/mol s, k_4 = 2.0 × 10^5 cm^2/mol s. Charging current: (a) –4.0 × 10^{-3}, (b) –10.0 × 10^{-3}, (c) –40.0 × 10^{-3}, (d) –80.0 × 10^{-3}, (e) –800.0 × 10^{-3} A/cm^2.

Charging of Electrode Interior

A threshold phenomenon has been proposed to initiate the effects reported by Fleischmann and Pons, i.e., contingent on achieving a degree of loading exceeding a certain critical value within a reasonably short period of time. In this section, we illustrate the interphase control vs. bulk transport control and show that an increase in the charging currents need not increase the level of electrode loading.

The coupling between interfacial processes and bulk transport admits, in principle, two modes of charging control. This is illustrated in Figs. 10, and *11*. To demonstrate the transition from interphase to transport control, we calculated the time dependences $\theta(t)$, $\eta(t)$ and the normalized amount of absorbed deuterium in terms of $Q(t) = \sum_{i=1}^{N} V_i \xi_i(t) / \sum_{i=1}^{N} V_i$ for the values of the diffusion coefficient differing by several orders of magnitude. As expected and illustrated in Fig. 10, the initial electrode response is independent of the diffusion coefficient. The quasi–steady state was established within 0.5 s. However, as soon as the build–up of absorbed deuterium has begun, θ and Q vary almost linearly with time. For an unrealistic value of the diffusion coefficient, (e.g., $\mathbf{D} = 10^{-4}$ cm^2 s^{-1}), θ and Q

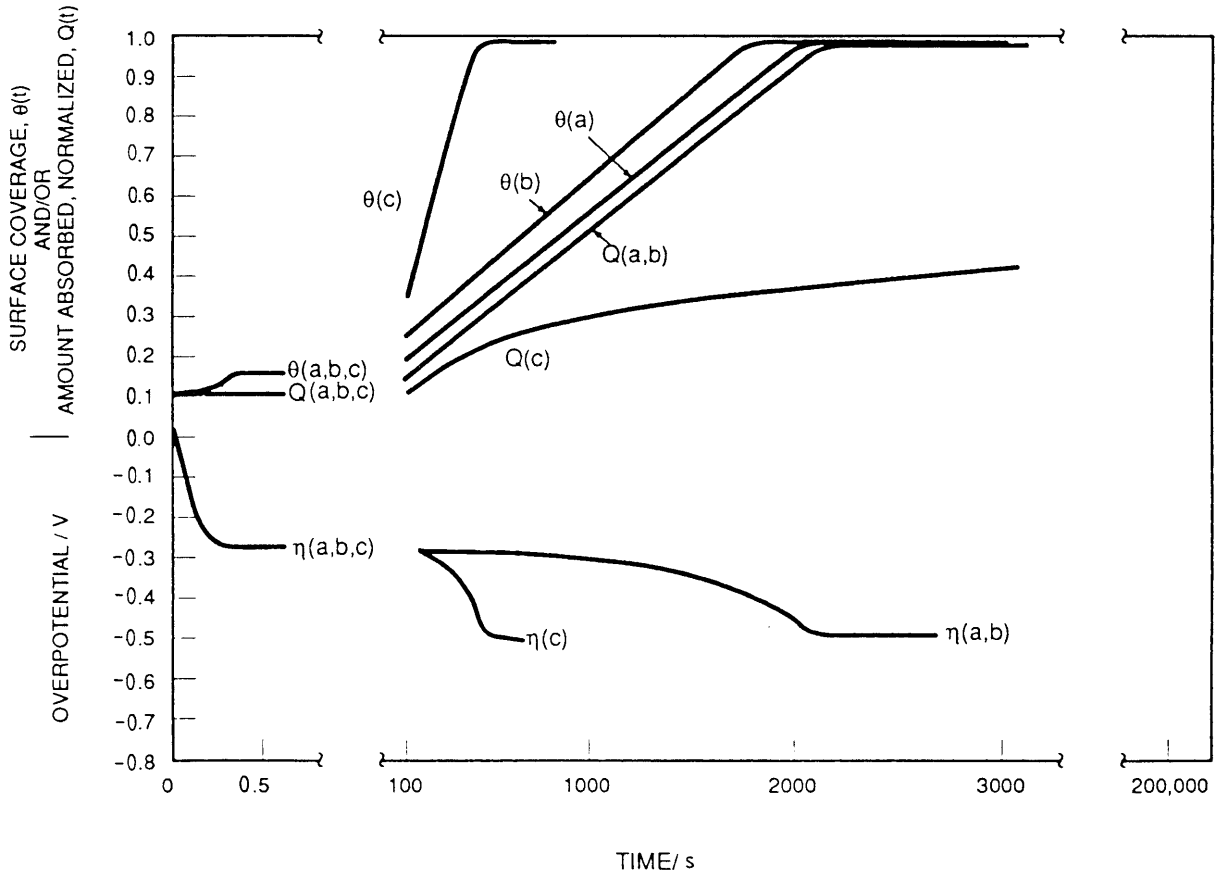

Figure A-10. Time dependent overpotential, η, surface coverage, θ, and normalized amount of absorption as a function of diffusion coefficient. (a) 10^{-4} cm^2/s; (b) 10^{-8} cm^2/s; (c) 10^{-10} cm^2/s. Charging current: 0.1 A/cm^2. Rate constants: $k_1 = 10^3$ cm^3/mol s, $k_2 = 10$ cm^3/mol s, $k_3 = 10^3$ cm^2/mol s, $k_4 = 2 \times 10^5$ cm^3/mol s.

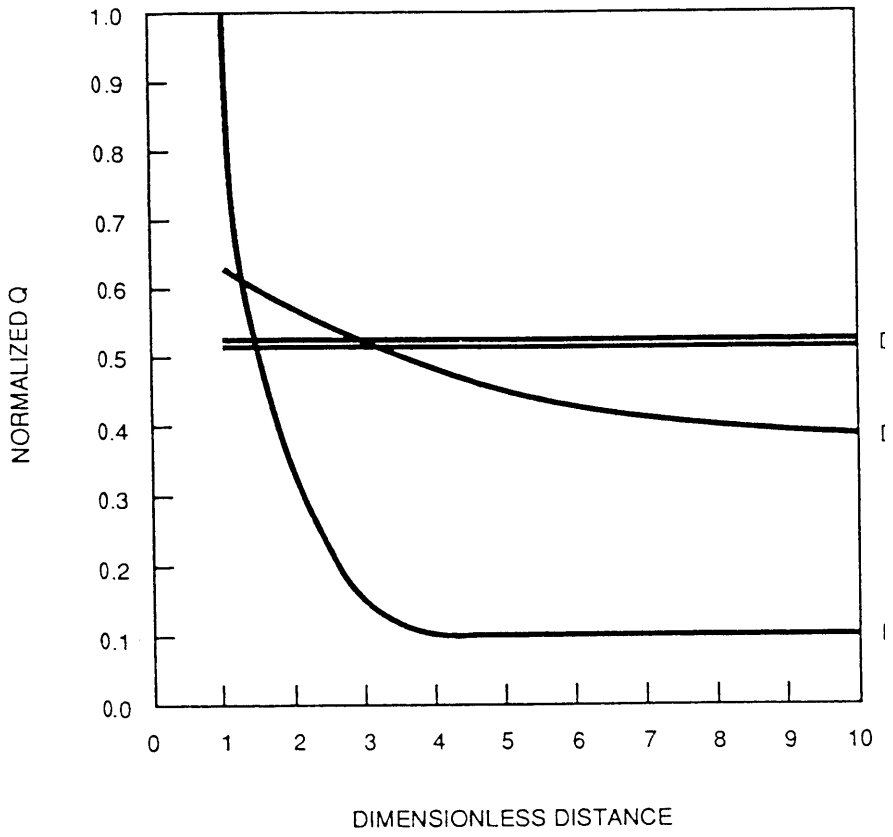

Figure A-11. Normalized amount of absorbed material as a function of distance. Diffusion coefficients (in cm^2/s) indicated; other data as in Fig. 10.

reached their limiting values almost simultaneously. This is consistent with interphase control. The transition to transport control, however, is not sharp and the electrode exhibits a mixed control for a substantial range of diffusion coefficients, e.g., $10^{-6} < \mathbf{D} < 10^{-8}$ cm^2 s^{-1}. In particular, for the set of input parameters in the example illustrated in Fig. 10, the electrode charging is under diffusion control only when $\mathbf{D} = 10^{-8}$ cm^2 s^{-1} or less. This transition from interphase to diffusion control manifests itself by an increase in the slope $d\theta/dt$ and a substantial delay in the achievement of full saturation of the electrode interior. The distribution of the filling of the available sites, Fig. 11, further illustrates the transition from the interphase to bulk diffusion control.

Another example of the effect of the complex interplay between the interphase processes at two charging current densities is shown in Fig. 12. Contrary to intuitive expectations that an increase in the charging currents should increase loading, the model predicts that, with a specific set of rate constants, a lower level of loading can result with no reduction in charging time observed.

CONCLUDING REMARKS

Qualitatively, the model reflects the complicated nature of the charging process. It indicates that difficulties may be encountered in controlling the charging process because of the large number of factors that may affect one or more of the interphase processes. Quantitative analysis could not be carried out because the relevant data were not available and the use of kinetic parameters associated

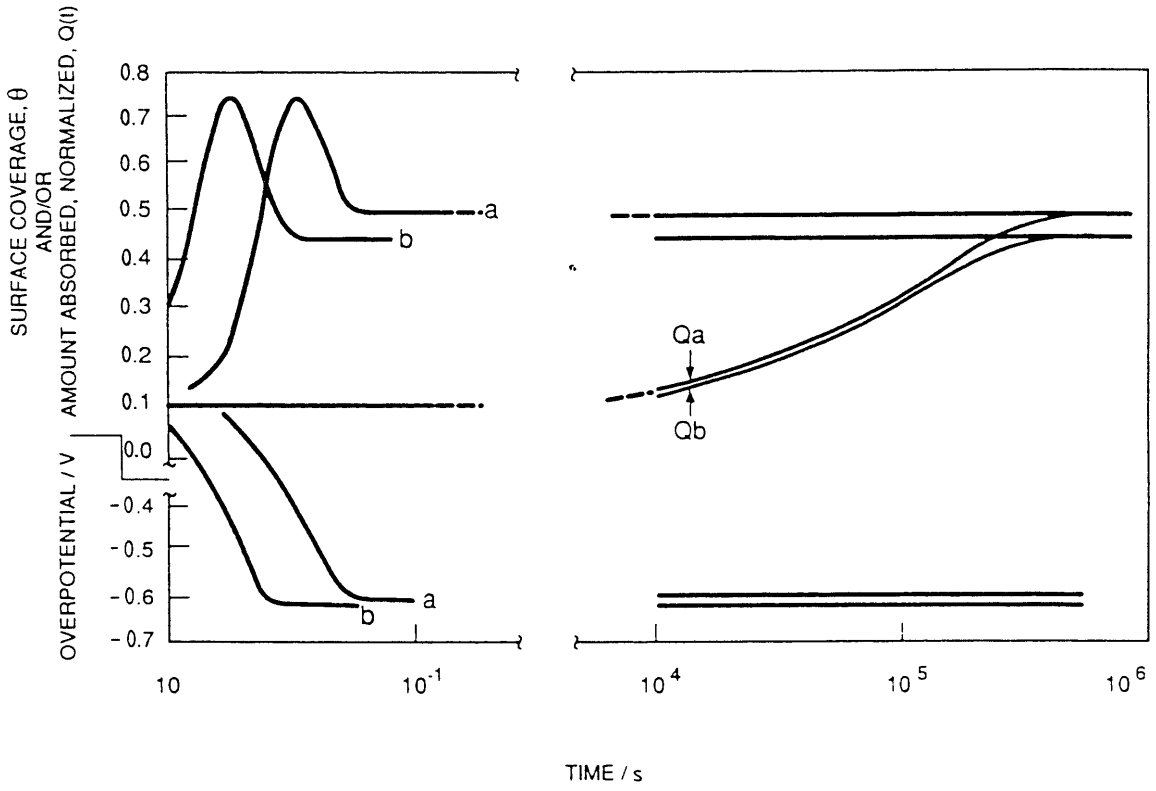

Figure A-12. Effect of charging current on electrode loading. (a) 0.05 A/cm^2; (b) 0.1 A/cm^2. Rate constants: $k_1 = 10^3$ cm^3/mol s; $k_2 = 10$ cm^3/mol s; $k_3 = 10^3$ cm^2/mol s; $k_4 = 2 \times 10^5$ cm^3/mol s.

with the hydrogen evolution reaction cannot be justified in view of recent results [23]. Other simplifications, e.g., the constancy of input parameters can be corrected (for example, a concentration dependent diffusion coefficient could be included). A more serious deficiency is the employment of the simplest interphase when, in fact, a supercharged region exists.

ACKNOWLEDGEMENT

The authors wish to thank Professors Fleischmann and Pons for helpful comments.

APPENDIX: DERIVATION OF EQNS. (17) AND (18)

The cross section of the rod of length L and radius r_0 is partitioned into N annular layers of thickness Δr. With the layers labeled from *1* to N from the outer surface to the center, respectively, the volume V_i of the ith layer and the interface surface $S_{i,i+1}$ between the ith and $(i + 1)$th layers are:

$$V_i = \pi(r_i^2 - r_{i+1}^2)L \tag{1A}$$

$$S_{i,i+1} = 2\pi r_{i+1}L \tag{2A}$$

where $r_i = (N - i + 1)\Delta r$. Consequently, the relevant surface to volume ratios are

$$\frac{S_{i\text{-}1,i}}{V_i} = \frac{2r_i}{r_i^2 - r_{r_{i+1}^2}} = \left(\frac{2r_i}{r_i + r_{i+1}}\right)\frac{1}{\Delta r} \tag{3A}$$

and

$$\frac{S_{i,i+1}}{V_i} = \frac{2r_{i+1}}{r_i^2 - r_{i+1}^2} = \frac{2r_i}{r_i + r_{i+1}}\left(1 - \frac{\Delta r}{r_i}\right)\frac{1}{\Delta r} \tag{4A}$$

Substitutions of these ratios into eqn. (8) yields

$$\frac{d\zeta_i}{dt} = d_d Z_m \Delta r\left(\frac{2r_i}{r_i + r_{i+1}}\right)\left[\frac{\zeta_{i\text{-}1} - 2\zeta_i + \zeta_{i+1}}{\Delta r^2} + \frac{1}{r_i}\left(\frac{\zeta_i - \zeta_{i+1}}{\Delta r}\right)\right] \tag{5A}$$

which, upon rearrangement becomes eqn. (19). The ratios given in eqns. (3A) and (4A) become, for $i = 1$

$$\frac{S_{0,1}}{V_i} = \left(\frac{2r_0}{2r_0 - \Delta r}\right)\frac{1}{\Delta r} \tag{6A}$$

and

$$\frac{S_{1,2}}{V_i} = \frac{2r_0}{2r_0 - \Delta r}\left(1 - \frac{\Delta r}{r_0}\right)\frac{1}{\Delta r} \tag{7A}$$

since $r_1 = r_0$ and $r_2 = r_0 - \Delta r$. Substitution of eqns. (6A) and (7A) into eqn. (17) yields eqn. (18).

The form of eqn. (5A) shows the relationship of eqn. (5A) to the diffusion equation written in cylindrical coordinates and approximated by finite differences. Generally, $k_d Z_m \Delta r$ would be identified with the diffusion coefficient and the ratio $2r_i/(r_i + r_{i+1})$ set equal to one as, in the limit, Δr approaches zero. However, here we retain the ratio as Δr is not necessarily small enough to take the limit, but do identify the diffusion coefficient as $k_d Z_m \Delta r$.

REFERENCES

1. J. Jorne, J. Electrochem. Soc., 137(1990) 369.
2. M. Fleischmann and S. Pons, J. Electroanal. Chem., 261(1989) 301; err. 263 (1989) 187. 3
3. Wagner, Z. Phys. Chem., A159 (1932)459; A193 (1944)386.
4. R. Fowler and E.A Guggenheim, Statistical Thermodynamics, Cambridge University Press Cambridge, 1949.
5. H.-G. Fritsche, Z. Naturforsch., 38a (1983)1118.
6. M. von Stackelberg and P. Ludwig, Z. Naturforsch., 19a (1964)93.
7. B. Dandapani and M. Fleischmann, J. Electroanal. Chem., 39(1972)323.
8. H. Brodowsky, Z. Phys. Chem., N.F., 44(1965)9.
9. R.M. Stoneham, Ber. Bunsenges. Phys. Chem., 76(1972)816.
10. J. Voelkl, Ber. Bunsenges. Phys. Chem., 76(1972)797.
11. E. Wicke and G.H. Nernst, Ber. Bunsenges. Phys. Chem., 68(1964)224.

12. R. Defay, I. Prigogine, A. Bellamans and D.H. Everett, Surface Tension and Adsorption, Longmans, Green and Co, Ltd., London, 1966.

13. H.–D. Ohlenbusch, Z. Elektrochem., 60(1955)603.

14. P. van Rysselberghe, in J.O'M. Bockris and B.E. Conway (Eds.), Moderns Aspects of Electrochemistry, Vol. 4, Plenum Press, New York, 1966, p. 1.

15. W. Auer and H.J. Grabke, Ber. Bunsenges. Phys. Chem., 78(1974)58.

16. E. Fromm, H. Uchida and B. Chelluri, Ber. Bunsenges. Phys. Chem., 87(1983)410.

17. S. Schuldiner and J.P. Hoare, J. Electrochem. Soc., 105(1958)278.

18. E. Gileadi and B.E. Conway, J. Chem. Phys., 39(1963)3420.

19. R.N. Iyer, H.W. Pickering and M. Zamanzadeh, J. Electrochem. Soc., 136(1989)2463.

20. R.M. Barrer and W. Jost, Trans. Faraday Soc., 45(1949)928.

21. M. Kuballa and B. Baranowski, Ber. Bunsenges Phys. Chem., 78(1974)335.

22. G. Sicking, M. Glugla and B. Huber, Ber. Bunsenges. Phys. Chem., 76(1972)418

23. D. Rolison and P.P. Trzaskoma, J. Electroanal. Chem., 287(1990)375.

24. S. Szpak, P.A. Mosier–Boss and J.J. Smith, unpublished results, 1990.

25. J.W. Davenport, G.J. Dienes and R.A. Johnson, Phys. Rev., 25(1982)2165.

26. W.H. Press and S.A. Teukolsky, Comput. Phys., May/June (1989)88.